Journal of Nuclear Medicine, published on May 1, 2020 as doi:10.2967/jnumed.119.233650

The Impact of Radiobiologically-Informed Dose Prescription on the Clinical Benefit of Yttrium-90 SIRT in Colorectal Cancer Patients

Elliot M. Abbott[1*], Nadia Falzone[1*], Boon Q. Lee[1], Christiana Kartsonaki[2], Helen Winter[3], Tessa A. Greenhalgh[3], Daniel R. McGowan[4], Nigar Syed[4], Ana M Denis-Bacelar[5], Philip Boardman[4], Ricky A. Sharma[6], Katherine A. Vallis[1**]

[1] Oxford Institute for Radiation Oncology, Department of Oncology, Oxford University, Oxford, UK

[2] Nuffield Department of Population Health, Oxford University, Oxford, UK

[3] Department of Oncology, Oxford University, Oxford, UK

[4] Department of Radiology, Oxford University Hospitals NHS Foundation Trust, Oxford, UK

[5] National Physical Laboratory, Teddington, UK

[6] Radiation Oncology, University College London, London, UK

***Joint first authors**

Elliot M. Abbott (PhD student)
T: +44 01865 225837 Email: Elliot.Abbott@oncology.ox.ac.uk

****Corresponding author:**
Katherine A. Vallis
T: +44 01865 225841 Email: katherine.vallis@oncology.ox.ac.uk

Oxford Institute for Radiation Oncology
Old Road Campus Research Building
Oxford, OX3 7DQ, UK

Running title: Radiobiological Dosimetry for SIRT

ABSTRACT

The purpose of this study was to establish the dose-response relationship of selective internal radiation therapy (SIRT) in patients with metastatic colorectal cancer (mCRC), when informed by radiobiological sensitivity parameters derived from mCRC cell lines exposed to yttrium-90 (^{90}Y). **Methods:** 23 mCRC patients with liver metastases refractory to chemotherapy were included. ^{90}Y bremsstrahlung SPECT images were transformed into dose maps assuming the local dose deposition method. Baseline and follow-up CT scans were segmented to derive liver and tumor volumes. Mean, median, and D_{70} (minimum dose to 70% of tumor volume) values determined from dose maps were correlated with change in tumor volume and vRECIST response using linear and logistic regression, respectively. Radiosensitivity parameters determined by clonogenic assays of mCRC cell lines HT-29 and DLD-1 after exposure to ^{90}Y or external beam radiotherapy (EBRT; 6MV photons) were used in biological effective dose (BED) calculations. **Results:** Mean administered radioactivity was 1469±428 MBq (847-2185 MBq), achieving a mean radiation absorbed tumor dose of 35.5±9.4 Gy and mean normal liver dose of 26.4±6.8 Gy. A 1.0 Gy increase in mean, median, and D_{70} absorbed dose was associated with reduction in tumor volume of 1.8%, 1.8%, and 1.5%, respectively, and increased probability of vRECIST response (odds ratio: 1.09, 1.09, and 1.10 respectively). Threshold mean, median and D_{70} doses for response were 48.3, 48.8, and 41.8 Gy respectively. EBRT-equivalent BEDs for ^{90}Y are up to 50% smaller than those calculated by applying protraction-corrected radiobiological parameters derived from EBRT alone. **Conclusion:** Dosimetric studies have assumed equivalence between ^{90}Y SIRT and EBRT, leading to inflation of BED for SIRT and possible under-treatment. Radiobiological parameters for ^{90}Y were applied to a BED model, providing a calculation method that has the potential to improve assessment of tumor control.

Key Words: Colorectal cancer; Liver metastases; SIRT; Yttrium-90; BED

INTRODUCTION

A multimodal approach to the control of liver-limited disease is important in the management of metastatic colorectal cancer (mCRC). Combination treatment incorporating external beam radiotherapy (EBRT) can be challenging as dose is constrained by hepatic radiosensitivity. An alternative is selective internal radiotherapy (SIRT), where yttrium-90 (^{90}Y)-radiolabeled microspheres are injected into the hepatic artery, lodge in abnormal tumor vessels and deliver β-radiation. Phase-3 trials (FOXFIRE, SIRFLOX, and FOXFIRE-Global) in patients with unresectable, chemo-refractory, liver-limited mCRC, have shown that SIRT plus chemotherapy improves control of liver disease but not overall survival (OS) (*1*). Except for first-line therapy, consensus guidelines recommend SIRT in combination with anticancer agents for mCRC liver tumors (*2*).

Current practice does not mandate personalized dose prescriptions for SIRT (*3*). Instead, the amount of administered radioactivity is usually based on body weight and height, ignoring variability in the accumulation of ^{90}Y and dose to individual tumors. A growing body of evidence shows that a dose-response relationship exists for SIRT. For example, the radiation dose delivered via SIRT correlates with change in total lesion glycolysis based on FDG-PET (*4-6*) and with tumor response defined by RECIST (*7,8*) or volumetric RECIST (vRECIST) criteria (*7,9*). Studies of ^{99m}Tc macroaggregated albumin (^{99m}Tc-MAA) imaging are inconsistent, some showing that it is predictive of ^{90}Y dose deposition and others not (*10*). Omission of individualized dosimetry may render the tumor absorbed radiation dose suboptimal and reduce the chance of response. This may be compounded if it is assumed that the biological response to ^{90}Y is like that of high energy photons. Given the difference in dose-rate (^{90}Y, 2–8Gy/day; EBRT, 1–5Gy/min) and quality of these two types of radiation, and the non-uniformity of dose distribution with SIRT, this assumption is unfounded (*11*).

Several investigators have argued for patient-specific SIRT dosimetry (*12*). Cremonesi *et al.* applied radiobiologic metrics derived from EBRT to inform SIRT treatment, recommending administration of higher amounts of radioactivity than given previously (*13*). Strigari *et al.* also drew on experience of the radiobiological effects of EBRT to predict the tumour control probability of

radionuclide therapy (*14,15*). Few studies have explored differences in the biological response to ^{90}Y SIRT compared to EBRT and the implications for treatment (*16,17*). We compared the radiobiological effects of ^{90}Y and high-energy photons in CRC cell lines using clonogenic assays (*16*). This highlighted that ^{90}Y and EBRT have markedly different effects that can be mainly ascribed to the continuous low dose rate of ^{90}Y radiation.

A tumor-by-tumor dosimetric analysis following SIRT in patients with mCRC to establish a radiobiological dose-response relationship is presented. Dose metrics were derived for each tumor: mean and median doses, D_{70} (minimum dose to 70% of tumor volume) and the relative standard deviation (RSD), a measure of dose heterogeneity. Statistical associations between these parameters and changes in tumor volume and vRECIST were explored. A dosimetric analysis that incorporated radiobiological parameters for ^{90}Y was undertaken and the clinical implications reviewed.

MATERIALS AND METHODS

Patient Selection

A review of 23 patients with CRC treated with ^{90}Y resin microspheres (SIR-Spheres®, Sirtex) at the Oxford Cancer Centre between November 2014 and October 2015 was conducted. Patients with inoperable chemorefractory liver metastases (96 tumors), no bone metastases, no previous SIRT, stable liver enzymes, no contraindications to angiography, and World Health Organization performance status >2 were included. Patient characteristics are shown in Table 1. Informed written consent, Institutional Review Board approval (Oxford University, PID12277), and Health Research Authority ethical approval (IRAS214611) were obtained.

SIRT Treatment

^{99m}Tc-MAA was used as a surrogate for ^{90}Y-microspheres to evaluate distribution and lung-shunt, but not as the basis for dosimetry. Angiography was performed to map vessels and, if there was extra-

hepatic shunting, coil embolization was used to redirect flow. ^{90}Y resin microspheres were injected through catheterization of the hepatic artery under fluoroscopic visualization. Administered ^{90}Y activity (847-2185 MBq, mean 1469±428 MBq) was prescribed according to the method used in the FOXFIRE trial based on body surface area (BSA), lung-shunt, and percentage tumor involvement (*1*).

Image Analysis

Triple-phase contrast-enhancement CT (GE LightSpeed VCT) and T2w fat-saturated MR images (GE Signa 3T) were acquired 11-48 days before treatment (baseline), SPECT-CT images were acquired 1-day post-treatment, and follow-up CT and MR images were acquired 8-12 weeks later. Manual registration of baseline CT and MR images to SPECT/CT was performed using HybridViewer software (v2.6F, HERMES). SPECT/CT scans were acquired on a dual-headed gamma camera (GE Discovery D670) by imaging bremsstrahlung radiation with energy window of 50-150keV using a medium-energy general-purpose collimator, 128×128-matrix, 90 views, 20s per view. The GE default settings were used for SPECT/CT data reconstruction (scatter-correction off, resolution-recovery on, attenuation-correction on). Images were processed using Xeleris (v3.0, GE) with the default ordered subset expectation maximization settings (OSEM; 2-iterations, 10-subsets).

Voxel-based gross tumor volumes were determined by cross-referencing CT sections with MR images to localize tumor boundaries and guide CT segmentation at baseline and 2-3-months follow-up. To assess outcome, response was based on vRECIST, comparing relative change in tumor volume defined as the ratio of the difference in tumor volume at baseline and after treatment to the baseline volume $\left(\frac{V_{followup}-V_{baseline}}{V_{baseline}}\right)$. Response criteria (CR, PR, stable disease and PR) were as was defined in (*9*).

Dosimetry

Liver and tumor segmentation was performed on contrast-enhanced baseline CT, treatment CT from SPECT/CT, and follow-up CT images. A cumulated activity matrix was derived by scaling the total

attenuation-corrected SPECT signal in the liver voxels plus the lung-shunt percentage to equal the cumulated administered activity assuming physical decay only. Absorbed dose for each voxel D_i was calculated for each voxel $\tilde{A}_i$ in the cumulated activity matrix using the local deposition method (equation 1) (*18*).

$$D_i = \tilde{A}_i \times S \quad (1)$$

The dose per unit cumulated activity, S (6.22 GyMBq^{-1}h^{-1}), was taken as a constant assuming that all the dose from ^{90}Y was absorbed within the SPECT voxel (4.42 mm water cube). Radiation spectra of ^{90}Y were from the unabridged decay data of the Medical Internal Radiation Dose tabulation (MIRD-RADTABS v2.2). Voxelised dose maps gave a distribution of doses in each tumor, which was summarized using dose-volume histograms (DVH). This was done using an in-house MATLAB® code, which was validated against replicated analysis with MIM SurePlan™ LiverY90 when SPECT counts were cumulated in the liver (3.6% larger *S*-value).

Radiobiological Models

The radiosensitivity parameters, α and β, which are the linear and quadratic terms of the linear-quadratic model (LQM), were previously determined for two CRC cell lines, DLD-1 and HT-29, exposed up to 30 Gy from ^{90}Y or 6MV photons (Table 2) (*16*). An α/β-ratio was established for a combined model of the two cell lines representing a range of CRC radiosensitivities. These experimentally-derived radiobiological parameters were used to determine BED, which allows comparison between different fractionation schedules or treatment modalities with specific α/β-ratios (*19*).

To compare the biological response of ^{90}Y versus EBRT, BEDs were calculated for ^{90}Y using radiosensitivity parameters from EBRT using either the conventional or a modified method proposed in (*16*). The modified method (equation 2), denoted $BED_{90Y,(\alpha/\beta)_{EBRT}}$, accounts for linear energy transfer (LET) and dose-rate effects of ^{90}Y radiation.

$$BED_{90Y,(\alpha/\beta)_{EBRT}} = D_{90\mathrm{Y}}\left(RBE_{max} + \frac{G_\infty D_{90Y}}{(\alpha/\beta)_{\mathrm{EBRT}}}\right) \quad (2)$$

where the cumulative dose of ^{90}Y radiation is $D_{90\mathrm{Y}}$, the maximum relative biological effectiveness $RBE_{max} = \alpha_{90\mathrm{Y}}/\alpha_{\mathrm{EBRT}}$, and G is the Lea-Catcheside dose-protraction factor, estimated for a fully-decayed radiation source as

$$G_{\infty} = \frac{T_{rep}}{T_{rep} + T_{phys}} \tag{3}$$

T_{rep} and T_{phys} are the sublethal damage repair half-time and radionuclide decay half-life, respectively. The radiobiological fitting parameters are summarized in Supplemental Table 1 (*16*). The conventional method, denoted $BED_{(\alpha/G\beta)_{EBRT}}$, uses *α/β*-ratios of EBRT adjusted only by the dose protraction factor (G_{∞}, equation 3) while assuming $\mathrm{RBE}_{\mathrm{max}}$=1. Voxelised liver BED maps of ^{90}Y were determined by converting the physical mean absorbed dose of each voxel to $BED_{90Y,(\alpha/\beta)_{EBRT}}$, using the α/β-ratio for the ^{90}Y mixed model.

Statistics

The R software package (v3.3.3, R Core Team) was used. Dose metrics (mean, standard deviation (SD), median, D_{70} and RSD of mean dose), were derived for each tumor from dose maps and used as explanatory variables in the regression analysis. Thresholds for each dose metric were determined based on the cutoff for decrease in tumor size. Linear regression was used to assess the relationship between dose and change in tumor volume. Logistic regression was used to assess the relationship between dose and response. Regressions were fitted using generalized estimating equations to account for tumors belonging to the same patient. Odds ratios (OR) are provided for the association between response and dose metrics. Tumors <1mL were not considered due to spatial resolution limitations of SPECT. α/β-ratios were derived from a linear mixed-effects model from experimental data. Calculated BED values were used in the regressions. Analyses were repeated with patients as the unit of analysis, with tumors grouped by patient.

RESULTS

Patients

Patient baseline characteristics are summarized in Table 1. Median OS was 10.5 months (one patient was alive at time of analysis). One patient experienced pain and nausea. No patient experienced liver decompensation.

Tumor Response and Absorbed Dose

Dosimetric information is shown for representative patients with partial and mixed responses (Figures 1, 2), and for patients that did not respond or progressed patient (Supplemental Figures 1, 2). Mean and median normal liver doses were 26.4±6.8 Gy (15.4-41.3) and 24.9 Gy (interquartile range, 22.3-30.6), respectively. Mean and median tumor doses were 35.5±9.4 Gy (2.2-84.8) and 32.9 Gy (interquartile range, 23.3-46.8), respectively.

Linear regression analysis showed that mean, median, and D_{70} dose values were statistically significantly correlated with a reduction in tumor volume of 1.8%/Gy ($p<0.005$), 1.8%/Gy, ($p<0.005$) and 1.5%/Gy ($p<0.01$), respectively (Figure 3). No tumor increased in volume after receiving mean, median, and D_{70} doses greater than 48.3, 48.8, and 41.8 Gy, respectively. The RSD of the voxelized-dose distribution, was not significantly correlated with tumor volume change ($p>0.5$). Exclusion of 47 small tumors (<10 mL) did not change the analysis; mean dose values were significantly correlated ($p=0.001$) with reduction in tumor volume (1.9%/Gy). Mean dose for tumors >10 mL was also significantly correlated ($p=0.044$) with reduction in tumor volume (1.8%/Gy). Large (>100 mL) and small (<10 mL) tumors were equally likely to respond to therapy. Linear regression analysis showed no appreciable correlation between baseline and follow-up tumor volume (Supplemental Figure 3).

vRECIST response after ^{90}Y SIRT for each tumor is shown (Figure 4). PR was achieved in 14% of tumors, SD in 63% and 23% showed PD. While there was a mixed response of tumors in individual patients, two (patients 15 and 18) did not respond to treatment, irrespective of tumor volume at baseline or dose. When evaluating PR as a measure of response against SD and PD, mean, median, and D_{70} tumor

doses were significantly correlated with vRECIST response (p<0.05, p<0.01, and p<0.0001 respectively) with ORs of 1.09, 1.09 and 1.10 respectively. RSD was not significantly correlated with response (p>0.5).

Radiobiological Models

Radiosensitivity parameters are summarized in Table 2. A mixed model, taking the mean of the α/β-ratio of two CRC cell lines, to represent variation in radiosensitivity in CRC, gave values of 8.02 and 226 Gy for EBRT and ^{90}Y respectively. BEDs were calculated on a voxel-by-voxel basis for each tumor using the mixed model for ^{90}Y. For the 96 tumors, the values of mean $BED_{90Y,(\alpha/\beta)_{EBRT}}$, median $BED_{90Y,(\alpha/\beta)_{EBRT}}$ and D_{70} $BED_{90Y,(\alpha/\beta)_{EBRT}}$ were 21.0 Gy (1.24–67.7 Gy), 20.9 Gy (1.22–65.3 Gy), and 17.4 Gy (1.13–55.5 Gy) respectively. Taking each tumor as the unit of analysis, the $BED_{90Y,(\alpha/\beta)_{EBRT}}$ metrics (mean, median, and D_{70}), correlated statistically significantly with change in tumor volume using linear regression analysis (p<0.01, p<0.005, p<0.01 respectively). With the patient as the unit of analysis, and when evaluating PR and stable disease versus PD, the mean, median, and D_{70} $BED_{90Y,(\alpha/\beta)_{EBRT}}$ metrics were significantly correlated with vRECIST response (p<0.01, p<0.01, p<0.0001 respectively) with ORs of 1.10, 1.10, and 1.09 respectively. RSD was not significantly correlated with response (p>0.5).

The relationship between ^{90}Y absorbed dose and BED for the conventional method $\left(BED_{(\alpha/G\beta)_{EBRT}}\right)$ was compared to the modified method ($BED_{90Y,(\alpha/\beta)_{EBRT}}$) (*16*). Figure 5 illustrates how misunderstandings can arise unless the differences in radiobiological effects of the two types of radiation are considered. For example, a physical dose from ^{90}Y irradiation of 48.3 Gy gives the same biological effective dose ($BED_{90Y(\alpha/\beta)_{EBRT}}$) as 32.5 Gy of ^{90}Y equivalent EBRT. When using EBRT α/β-ratios, this was shown to be equivalent to a BED ($BED_{(\alpha/G\beta)_{EBRT}}$) of 54.9 Gy.

DISCUSSION

The success of EBRT is attributable to an understanding of the absorbed dose-response relationship, encapsulated by the LQM. This relationship has been adopted for radionuclide therapy without the support of experimental data to illuminate the specific biological effects of radioisotopes. Differences in biological effects result in variable RBE, despite the same amount of energy absorbed per unit mass. For this reason, the modified BED equation (equation 2) that accounts for dose-rate and LET was used. Cell repopulation effects play a role in BED modeling due to the timescale of the treatment, but limited data exist for ^{90}Y SIRT. Because cell-doubling times would be extrapolated from EBRT, repopulation was excluded from the BED model here.

There are no standard methods for ^{90}Y SIRT dosimetry reporting. Best practice is to follow published guidelines and report the protocols followed to enable critical evaluation of data (*20*). This allows compilation of dose-effect relationships in the absence of large multicenter trials, and informs future studies focusing on delivering tumoricidal radiation doses.

In this study, spatial dose distribution was consolidated into a DVH and tumors were considered individually. A caveat is that spatial information is lost, and so the mean absorbed dose of a tumor does not always reflect intratumoral dose heterogeneity. Therefore we also examined the association between change in tumor volume and median and D_{70} values (Figure 3). Threshold mean, median, and D_{70} doses of 48.3, 48.8, and 41.8 Gy respectively are reasonably consistent with the mean dose of 29.8 Gy and D_{70} of 42.3 Gy reported by Fowler *et al* (*7*), the average dose of about 50 Gy reported by Willowson *et al* (*21*), an average dose greater than 66 Gy (95% CI 32–159 Gy) noted by Flamen *et al* (*4*) and results from a prospective study (*6*) which reported a dose of 51±28 Gy as the minimum tumor absorbed dose needed to reduce total lesion glycolysis by >50%. Levillain *et al*. noted that a significantly longer OS was observed in patients with lesions achieving a mean dose >39 Gy (*5*). However, direct comparison with these studies is limited as, unlike the current study, they used ^{99m}Tc-MAA SPECT or ^{90}Y PET imaging. As reported by others, efficacy in patients receiving glass microspheres or EBRT resulted in tumor α-values that were at least an order of magnitude smaller than found in clonogenic experiments (≈0.2 Gy^{-1}) (*22*). These

unexpectedly low values were attributed to being "effective radiosensitivity" and considered to be pragmatic input figures for radiobiological modelling (*22*). Notably, an effective RBE_{max} of 0.4 was reported, which agrees with 0.56 in the mixed model presented here.

Despite using the same activity calculation scheme, the median OS for the combined FOXFIRE, SIRFLOX, and FOXFIRE-Global analysis was 12.1 months longer than this patient group. The combined analysis patients achieved 68% CR plus PR whereas in the current group no patient had CR and 14% had PR, suggesting they had more advanced disease. Indeed the combined analysis patients had a lower rate of extrahepatic metastases and no prior chemotherapy. If a response threshold appears to be strongly dependent upon tumor size, it could indicate that target tumor absorbed dose may be modified to increase response or, if dose heterogeneity was a prognostic factor, EBRT could be considered to boost low-dose regions. Bhooshan *et al*. found that pre-treatment volume was a significant predictor of SD or PR using volumetric response criteria (*23*). Therefore, we evaluated baseline tumor volume as a predictor of tumor response but found there was no statistically significant correlation between baseline and change in tumor volume. It is documented that absorbed dose heterogeneity in tumors leads to a lack of response (*21*). We evaluated RSD as a measure of dose heterogeneity. Linear regression analysis showed no correlation between RSD and change in volume. Absorbed dose heterogeneity at the microscopic level would suggest more cells received over- or under-dosing than could be captured by a SPECT voxel and would broaden the DVH. The differences in response noted in individual patients could be the result of microscopic dose heterogeneity, phenotype, or molecular pathologic differences between tumors.

Image reconstruction settings affect these results. As the bremsstrahlung SPECT reconstruction was performed without scatter correction, the images had depreciated contrast that likely underestimated tumor doses while overestimating non-tumor doses. Scatter correction strategies should be applied to ^{90}Y SPECT imaging. Phantom studies on the same type of SPECT scanner as used here, indicate that OSEM (5 iterations, 15 subsets) with Monte Carlo collimator modeling improved contrast recovery (*24*). This software was unavailable for this study. Porter *et al*. showed a 14.1 mL sphere had about 20% smaller contrast recovery than a 33.5 mL sphere. As recovery correction was not performed and varies with size,

smaller tumors would be biased to have artificially lower doses. Partial volume corrections were not included in this cohort. Low contrast recovery has been observed in spheres less than 4.2 mL (20 mm diameter) (*21,24*) and the partial volume effect has been shown to result in activity recovery of about 20% for small lesions (*25,26*). For this reason, tumors <10 mL were analyzed separately. When small tumors were omitted, overall correlations were unchanged.

To achieve tumoricidal doses, understanding the biological effect of dose is necessary. Radiobiological models such as BED can be used to plan re-treatments or additional treatments such as EBRT to under-treated tumors. BED calculations using ^{90}Y SIRT patient data have not previously been performed using radiosensitivity parameters determined experimentally from CRC cell lines. It is usually assumed that the α/β-ratios of ^{90}Y and EBRT are related and simply adjusted for the protracted delivery of dose with ^{90}Y (*8,14*). This has been shown to not be the case (Table 2) and a formula relating the BED of different radiation modalities was derived (*16*).

Toxicity was modest in this cohort, consistent with a recent study showing no evidence of radiation-induced hepatitis following SIRT (*27*). The FOXFIRE, SIRFLOX, and FOXFIRE-Global clinical trials found that ^{90}Y SIRT improved local control but did not improve OS (*28*). This could be due to dose heterogeneity (*3,8,11,12*) or low dose rate (*13,15*). However, our results indicate that there was no statistically significant correlation between change in tumor volume and bremsstrahlung SPECT-based dose heterogeneity. Although we cannot discount the effect of low dose rate, the main finding when applying experimentally determined α/β-ratios is that physical ^{90}Y doses achieved (40-60 Gy in tumor), are biologically equivalent to EBRT doses that are 20-30% lower. If an EBRT BED of approximately 70 Gy is required for liver lesions, a BED of about 50 Gy delivered by ^{90}Y SIRT would be less effective.

CONCLUSION

Dosimetry provides patient-specific information for optimal treatment. Radiobiological models can aid in delivering efficacious dose to tumour while limiting dose to healthy tissue. BED calculations

based on measured CRC radiosensitivity are lower than conventionally-calculated BEDs. Conventionally calculated ^{90}Y doses may sometimes be insufficient to achieve tumor control.

DISCLOSURE

No conflicts of interest.

ACKNOWLEDGEMENTS

The authors thank Drs. Glenn Flux and Allison Craig for discussions regarding dosimetry. This research was supported by grants from Cancer Research UK (C5255/A15935) and the Medical Research Council (MC-PC-12004).

KEY POINTS

QUESTION: Does the inclusion of radiobiological parameters specific to a therapeutic radionuclide affect the dose prescription?

PERTINENT FINDINGS: Mean, median, and D_{70} dose values correlated with change in tumor volume and vRECIST response. BEDs for ^{90}Y are up to 50% smaller than those conventionally-calculated by radiobiological parameters derived from EBRT adjusted for protraction effects only.

IMPLICATIONS FOR PATIENT CARE: Conventionally-calculated ^{90}Y doses may sometimes be insufficient to achieve tumor control.

REFERENCES

1. Wasan HS, Gibbs P, Sharma NK, et al. First-line selective internal radiotherapy plus chemotherapy versus chemotherapy alone in patients with liver metastases from colorectal cancer (FOXFIRE, SIRFLOX, and FOXFIRE-Global): a combined analysis of three multicentre, randomised, phase 3 trials. *Lancet Oncol.* 2017;18:1159-1171.

2. Kennedy A, Brown DB, Feilchenfeldt J, et al. Safety of selective internal radiation therapy (SIRT) with yttrium-90 microspheres combined with systemic anticancer agents: expert consensus. *J Gastrointest Oncol.* 2017;8:1079-1099.

3. Kao YH, Hock Tan AE, Burgmans MC, et al. Image-guided personalized predictive dosimetry by artery-specific SPECT/CT partition modeling for safe and effective ^{90}Y radioembolization. *J Nucl Med.* 2012;53:559-566.

4. Flamen P, Vanderlinden B, Delatte P, et al. Multimodality imaging can predict the metabolic response of unresectable colorectal liver metastases to radioembolization therapy with yttrium-90 labeled resin microspheres. *Phys Med Biol.* 2008;53:6591-6603.

5. Levillain H, Duran Derijckere I, Marin G, et al. ^{90}Y-PET/CT-based dosimetry after selective internal radiation therapy predicts outcome in patients with liver metastases from colorectal cancer. *EJNMMI Res.* 2018;8:60.

6. van den Hoven A, Rosenbaum C, Elias S, et al. Insights into the dose-response relationship of radioembolization with resin yttrium-90 microspheres: a prospective cohort study in patients with colorectal cancer liver metastases. *J Nucl Med.* 2016;57:1014-1019.

7. Fowler KJ, Maughan NM, Laforest R, et al. PET/MRI of hepatic ^{90}Y microsphere deposition determines individual tumor response. *Cardiovasc Intervent Radiol.* 2016;39:855-864.

8. Strigari L, Sciuto R, Rea S, et al. Efficacy and toxicity related to treatment of hepatocellular carcinoma with ^{90}Y-SIR spheres: radiobiologic considerations. *J Nucl Med.* 2010;51:1377-1385.

9. Chapiro J, Duran R, Lin M, et al. Early survival prediction after intra-arterial therapies: a 3D quantitative MRI assessment of tumour response after TACE or radioembolization of colorectal cancer metastases to the liver. *Eur Radiol.* 2015;25:1993-2003.

10. Wondergem M, Smits ML, Elschot M, et al. ^{99m}Tc-macroaggregated albumin poorly predicts the intrahepatic distribution of ^{90}Y resin microspheres in hepatic radioembolization. *J Nucl Med.* 2013;54:1294-1301.

11. Hogberg J, Rizell M, Hultborn R, et al. Increased absorbed liver dose in selective internal radiation therapy (SIRT) correlates with increased sphere-cluster frequency and absorbed dose inhomogeneity. *EJNMMI Phys.* 2015;2:10.

12. Tong AK, Kao YH, Too CW, Chin KF, Ng DC, Chow PK. Yttrium-90 hepatic radioembolization: clinical review and current techniques in interventional radiology and personalized dosimetry. *Br J Radiol.* 2016;89:20150943.

13. Cremonesi M, Ferrari M, Bartolomei M, et al. Radioembolisation with ^{90}Y-microspheres: dosimetric and radiobiological investigation for multi-cycle treatment. *Eur J Nucl Med Mol Imaging.* 2008;35:2088-2096.

14. Strigari L, Benassi M, Chiesa C, Cremonesi M, Bodei L, D'Andrea M. Dosimetry in nuclear medicine therapy: radiobiology application and results. *Q J Nucl Med Mol Imaging.* 2011;55:205-221.

15. Strigari L, Konijnenberg M, Chiesa C, et al. The evidence base for the use of internal dosimetry in the clinical practice of molecular radiotherapy. *Eur J Nucl Med Mol Imaging.* 2014;41:1976-1988.

16. Lee BQ, Abbott EM, Able S, et al. Radiosensitivity of colorectal cancer to ^{90}Y and the radiobiological implications for radioembolisation therapy. *Phys Med Biol.* 2019;64:135018.

17. Gholami YH, Willowson KP, Forwood NJ, et al. Comparison of radiobiological parameters for ^{90}Y radionuclide therapy (RNT) and external beam radiotherapy (EBRT) in vitro. *EJNMMI Phys.* 2018;5:18.

18. Pasciak AS, Bourgeois AC, Bradley YC. A comparison of techniques for ^{90}Y PET/CT image-based dosimetry following radioembolization with resin microspheres. *Front Oncol.* 2014;4:121.

19. Dale RG, Jones B. The assessment of RBE effects using the concept of biologically effective dose. *Int J Radiat Oncol Biol Phys.* 1999;43:639-645.

20. Giammarile F, Bodei L, Chiesa C, et al. EANM procedure guideline for the treatment of liver cancer and liver metastases with intra-arterial radioactive compounds. *Eur J Nucl Med Mol Imaging.* 2011;38:1393-1406.

21. Willowson KP, Hayes AR, Chan DLH, et al. Clinical and imaging-based prognostic factors in radioembolisation of liver metastases from colorectal cancer: a retrospective exploratory analysis. *EJNMMI Res.* 2017;7:46.

22. Chiesa C, Mira M, Maccauro M, et al. Radioembolization of hepatocarcinoma with ^{90}Y glass microspheres: development of an individualized treatment planning strategy based on dosimetry and radiobiology. *Eur J Nucl Med Mol Imaging.* 2015;42:1718-1738.

23. Bhooshan N, Sharma NK, Badiyan S, et al. Pretreatment tumor volume as a prognostic factor in metastatic colorectal cancer treated with selective internal radiation to the liver using yttrium-90 resin microspheres. *J Gastrointest Oncol.* 2016;7:931-937.

24. Porter CA, Bradley KM, Hippelainen ET, Walker MD, McGowan DR. Phantom and clinical evaluation of the effect of full Monte Carlo collimator modelling in post-SIRT yttrium-90 Bremsstrahlung SPECT imaging. *EJNMMI Res.* 2018;8:7.

25. Siman W, Mikell JK, Kappadath SC. Practical reconstruction protocol for quantitative ^{90}Y bremsstrahlung SPECT/CT. *Med Phys.* 2016;43:5093.

26. Willowson KP, Tapner M, Team QI, Bailey DL. A multicentre comparison of quantitative (90)Y PET/CT for dosimetric purposes after radioembolization with resin microspheres : The QUEST Phantom Study. *Eur J Nucl Med Mol Imaging.* 2015;42:1202-1222.

27. Justinger C, Gruden J, Kouladouros K, et al. Histopathological changes resulting from selective internal radiotherapy (SIRT). *J Surg Oncol.* 2018;117:1084-1091.

28. Gnesin S, Canetti L, Adib S, et al. Partition model-based ^{99m}Tc-MAA SPECT/CT predictive dosimetry compared with ^{90}Y TOF PET/CT posttreatment dosimetry in radioembolization of hepatocellular carcinoma: a quantitative agreement comparison. *J Nucl Med.* 2016;57:1672-1678.

FIGURES

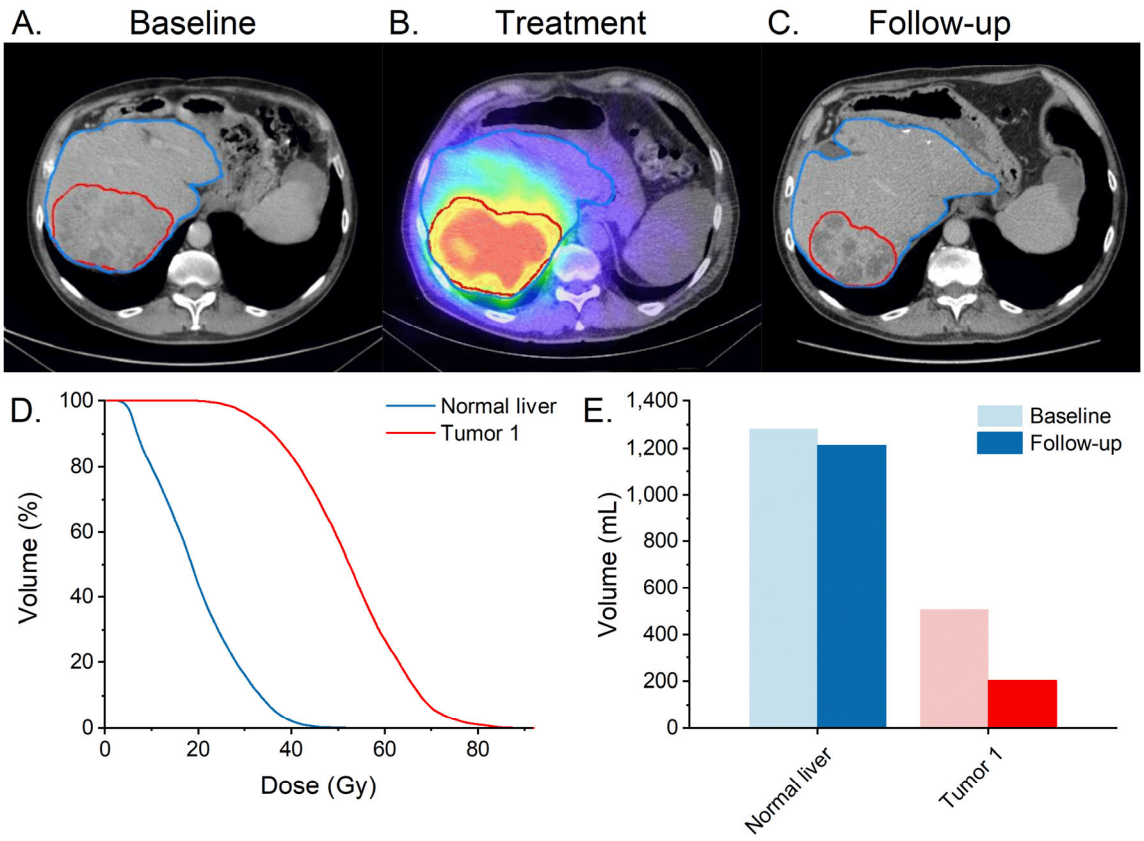

FIGURE 1. Patient 2 (75 y, 1.78 m^2 BSA): rectal cancer with pulmonary and liver metastases, treated by hepatic resection and chemotherapy. (A) Baseline imaging acquired 15-days prior to SIRT. ^{99m}Tc-MAA, angiography and coil embolisation were performed, achieving 16.8% lung shunt. ^{90}Y microspheres (1562 MBq) were administered. (B) SPECT/CT 1-day post-SIRT demonstrating a favorable distribution of ^{90}Y in tumor. (C) CT images 80-days following SIRT revealed PR, but significant extra-hepatic disease remained. (D) DVH of absorbed doses in normal liver and tumor. (E) Volumetric analysis indicated tumor response.

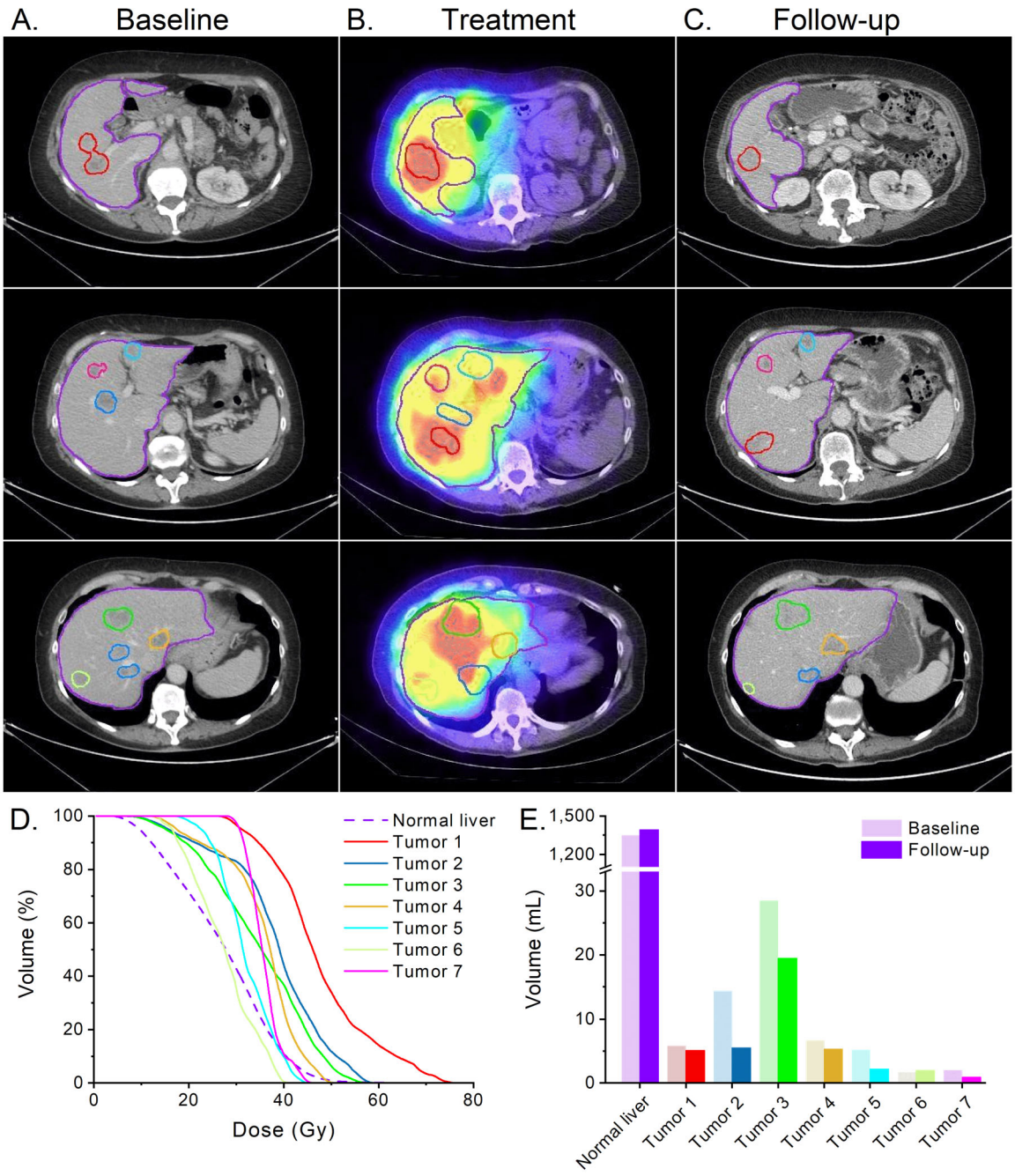

FIGURE 2. Patient 14 (66y, 1.70m^2 BSA): liver, ovarian, and pulmonary metastases, treated by resection of descending/sigmoid colon adenocarcinoma and three courses of chemotherapy. (A) Baseline CT acquired 27-days before SIRT. ^{99m}Tc-MAA, angiography and coil embolization were performed, achieving 0% lung shunt. ^{90}Y microspheres were administered in two injections of 939 MBq, (B) SPECT/CT 1-day post-SIRT demonstrated variable accumulation in tumors. (C) CT at 74-days revealed

PR in some lesions. (D) DVH of liver and tumor absorbed doses reflect variable uptake in tumor. (E) Tumor response was variable.

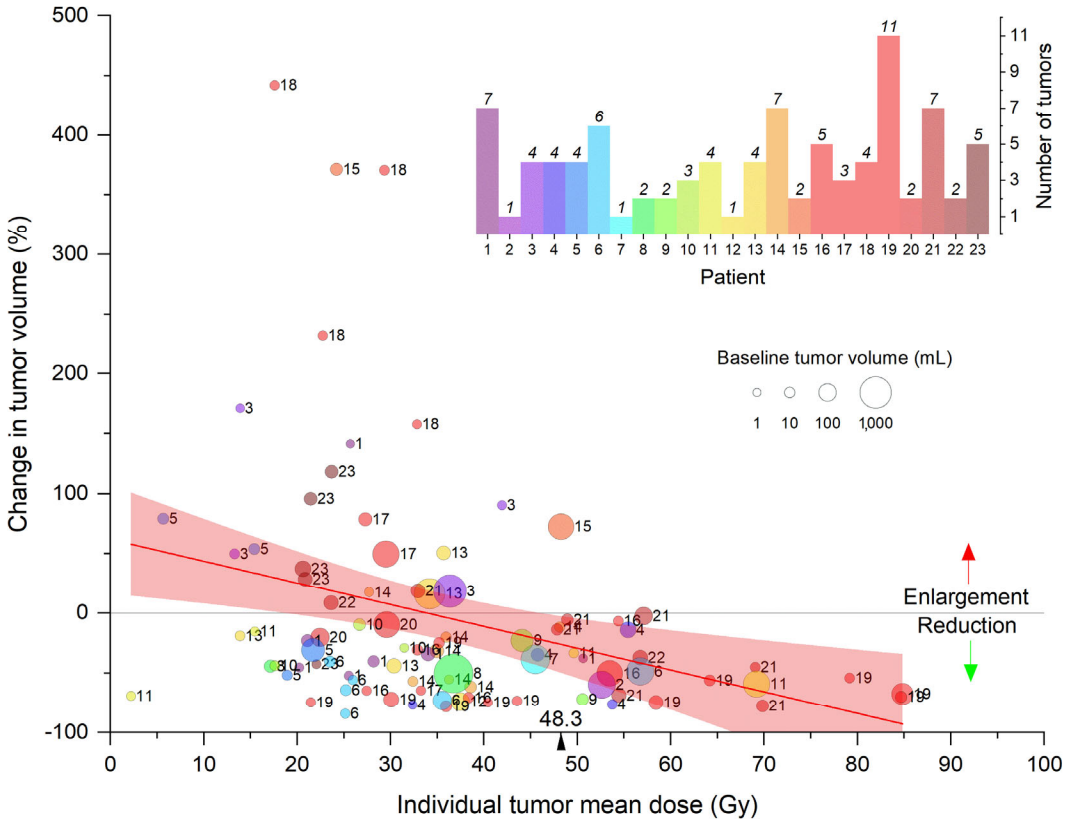

FIGURE 3. Relationship between change in tumor volume and mean dose. The tumors of each patient are depicted in the same color and numbered. Data points above the horizontal grey line indicate tumor growth at follow-up, points below denote tumor shrinkage. Linear regression analysis (red line, 95% CI of best fit) shows a reduction in tumor volume of 1.8% per 1.0 Gy of absorbed dose (95% CI 0.7–3.0%, $p<0.005$, $R^2=0.102$). All tumors that received ≥48.3 Gy reduced in size.

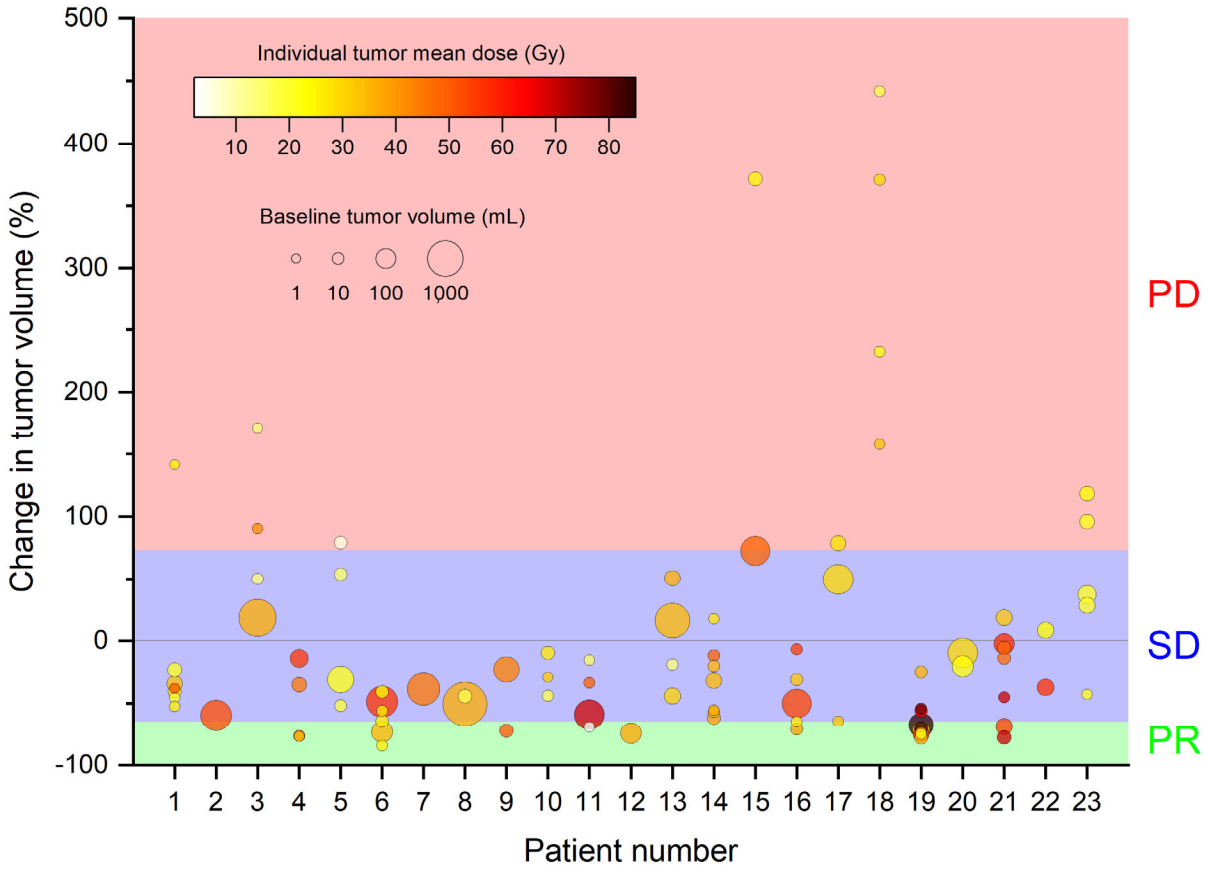

FIGURE 4. vRECIST response as a function of dose for each tumor. No tumors showed CR. All tumors that showed a reduction in volume of at least 65% were PR. Tumors that grew by at least 73% were termed PD. Tumors not meeting these criteria were designated as stable disease (SD).

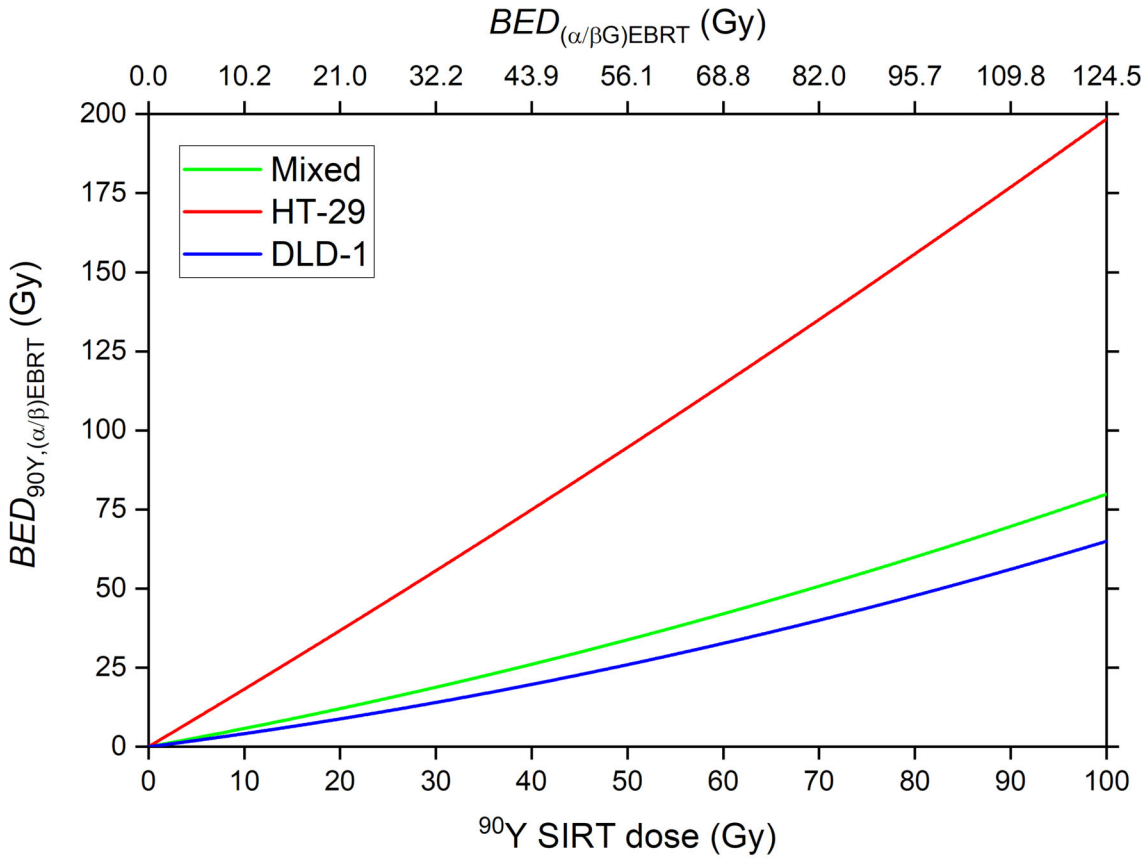

FIGURE 5. Relationship between physical ^{90}Y dose and BED. BED was calculated using experimentally-derived parameters for DLD-1 and HT-29 cell lines and a mixed model of both cell lines (Supplemental Table 1). BED as given in equation 2 (y-axis) was compared to BED (top x-axis) calculated using the conventional assumption RBE_{max}=1.

TABLE 1 Patient characteristics

Characteristic	**N (%)** or **mean ± standard deviation**
Gender	
Male	14 (61%)
Female	9 (39%)
Age (y)	63±11
Primary site	
Cecal	1 (4%)
Colon	10 (43%)
Rectum	12 (52%)
*Baseline tumor burden (%)	19±16
<25%	17 (74%)
25-50%	5 (22%)
>50%	1 (4%)
Baseline individual tumor volume (mL)	107±284
†Baseline total tumor volume (mL)	436±471
Extrahepatic metastases	
Lung	12 (52%)
Mediastinum	2 (9%)
Lymph node	7 (30%)
Prior systemic therapies	
1 line	2 (9%)
2 lines	13 (57%)
3 lines	8 (35%)
Prior EBRT	2 (9%)
Hepatectomy	7 (30%)
Ras mutation	7 (30%)
SIRT treatment	
Coil embolisation	22 (96%)
Number of tumors	96
Number of tumors considered per patient	4.0±2.4
Administered activity (MBq)	1469±428

* Total tumor volume/liver volume, from baseline CT imaging

†Sum volume of tumors at baseline based on CT contours

TABLE 2 α, β (corrected for indefinite exposure), and α/β-values for DLD-1 and HT-29 cell lines adopted from Lee *et al* (*16*) compared to a mixed model after exposure to 6 MV photons (EBRT) or ^{90}Y. Range shown in brackets represents the 95% confidence interval of the estimated parameter.

Cell line	Radiation source	α (Gy^{-1})	β (Gy^{-2})	α/β (Gy)
DLD-1	EBRT	0.273	0.0189	14.4
		[0.187–0.359]	[0.00970–0.0282]	[3.15–25.7]
	^{90}Y	0.106	0.000716	148
		[0.075–0.137]	[-0.00008–0.00151]	[-56.3–353]
HT-29	EBRT	0.050	0.0276	1.81
		[0.008–0.092]	[0.0230–0.0323]	[0.0247–3.60]
	^{90}Y	0.090	0.000092	979
		[0.063–0.116]	[-0.001018–0.001201]	[-6911–8861]
Mixed model	EBRT	0.176	0.0219	8.02
		[0.0092–0.256]	[0.0136–0.0304]	[1.39–14.6]
	^{90}Y	0.0977	0.00043	226
		[0.075–0.12]	[-0.00015–0.001]	[-129–582]

SUPPLEMENTAL MATERIAL

Supplemental Table 1: Comparison of ^{90}Y SIRT radiobiological modelling parameters derived for each cell line using LQM fitted parameters in Table 2. The RBE_{max} and Lea-Catcheside factor of 6-day exposure G_6 values were extracted from LQM fit parameters of experimental data. The repair half-time T_{rep} was determined using supplemental equation S4 from Lee *et al. (16)* to correct for the experimental limitations of a 6-day exposure rather than the indefinite exposure which is given for ^{90}Y SIRT. The indefinite exposure-corrected Lea-Catcheside factor G_∞ was determined using equation 3. The last column shows the $(\alpha/\beta)_{90Y}$ for indefinite exposure and is given in Table 2. The range shown within brackets represents the 95% confidence interval of the estimated parameter.

Cell line	$\boldsymbol{RBE_{max}}$ ($\boldsymbol{\alpha_{90Y}/\alpha_{EBRT}}$)	$\boldsymbol{G_6}$ ($\boldsymbol{\beta_{90Y}/\beta_{EBRT}}$)	$\boldsymbol{T_{rep}}$ (h)	$\boldsymbol{G_\infty}$	$\boldsymbol{\alpha_{90Y}/G_\infty\beta_{EBRT}}$ (Gy)
DLD-1	0.388 [0.221–0.555]	0.0577 [-0.0123–0.1277]	2.51 [-0.67–5.69]	0.0377 [-0.0102–0.0856]	148 [-56.3–353]
HT-29	1.800 [0.198–3.402]	0.0051 [-0.0351–0.0453]	0.21 [-1.48–1.90]	0.0033 [-0.0230–0.0296]	979 [-6911–8861]
Mixed model	0.554 [0.145–0.963]	0.0300 [-0.0117–0.0718]	1.28 [1.27–1.29]	0.0196 [0.0195–0.0198]	226 [-129–582]

16. Lee BQ, Abbott EM, Able S, et al. Radiosensitivity of colorectal cancer to ^{90}Y and the radiobiological implications for radioembolisation therapy. *Phys Med Biol.* 2019;64:135018.

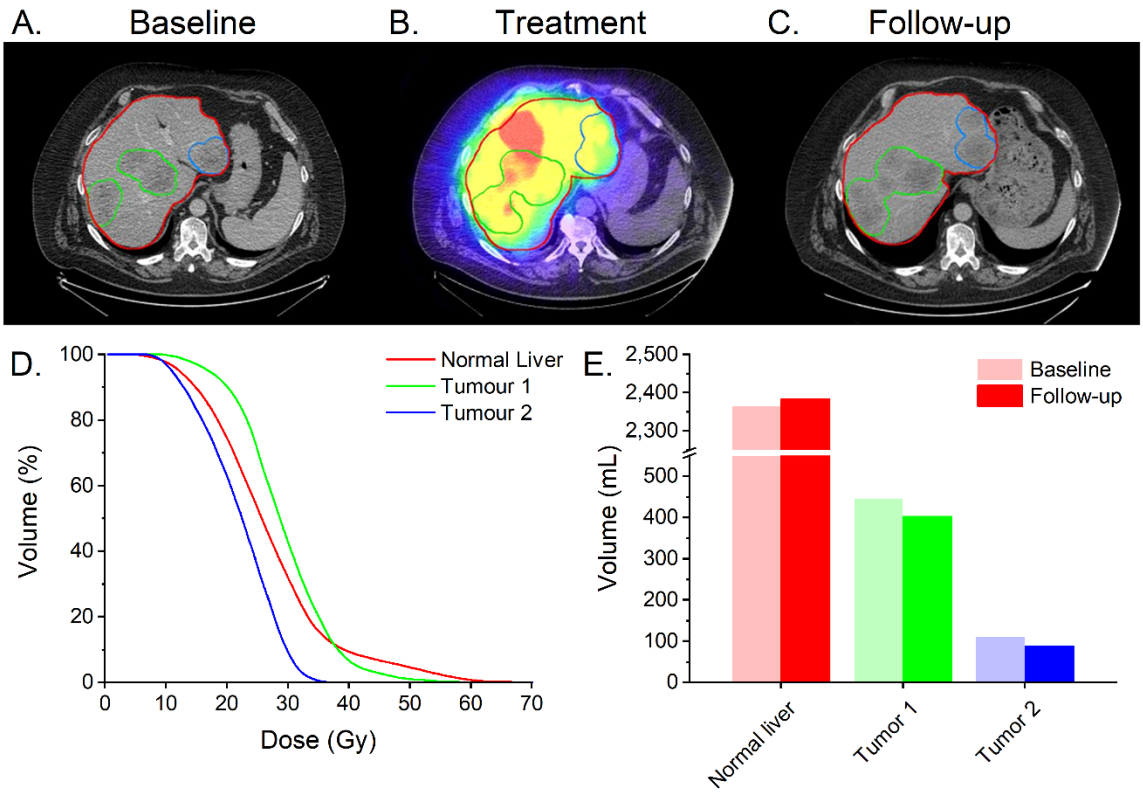

Supplemental Figure 1: Patient 20 (63 y, 2.74 m^2 BSA): rectal carcinoma with Ras mutation, mediastinal metastasis, and lymphadenopathy. The primary tumor was resected and the patient received one line of prior chemotherapy. (A) Baseline imaging acquired 13 days prior to SIRT confirmed PD. ^{99m}Tc-MAA, angiography and coil embolisation were performed to achieve 4.7% lung shunt. ^{90}Y microspheres were administered in a single injection of 1863 MBq. (B) SPECT/CT one day post-SIRT demonstrated suboptimal uptake distribution. (C) CT imaging 74 days following SIRT revealed no response. (D) DVH of absorbed doses to the normal liver was comparable to each of the two tumors. (E) Volumetric reponse illustrates stable disease.

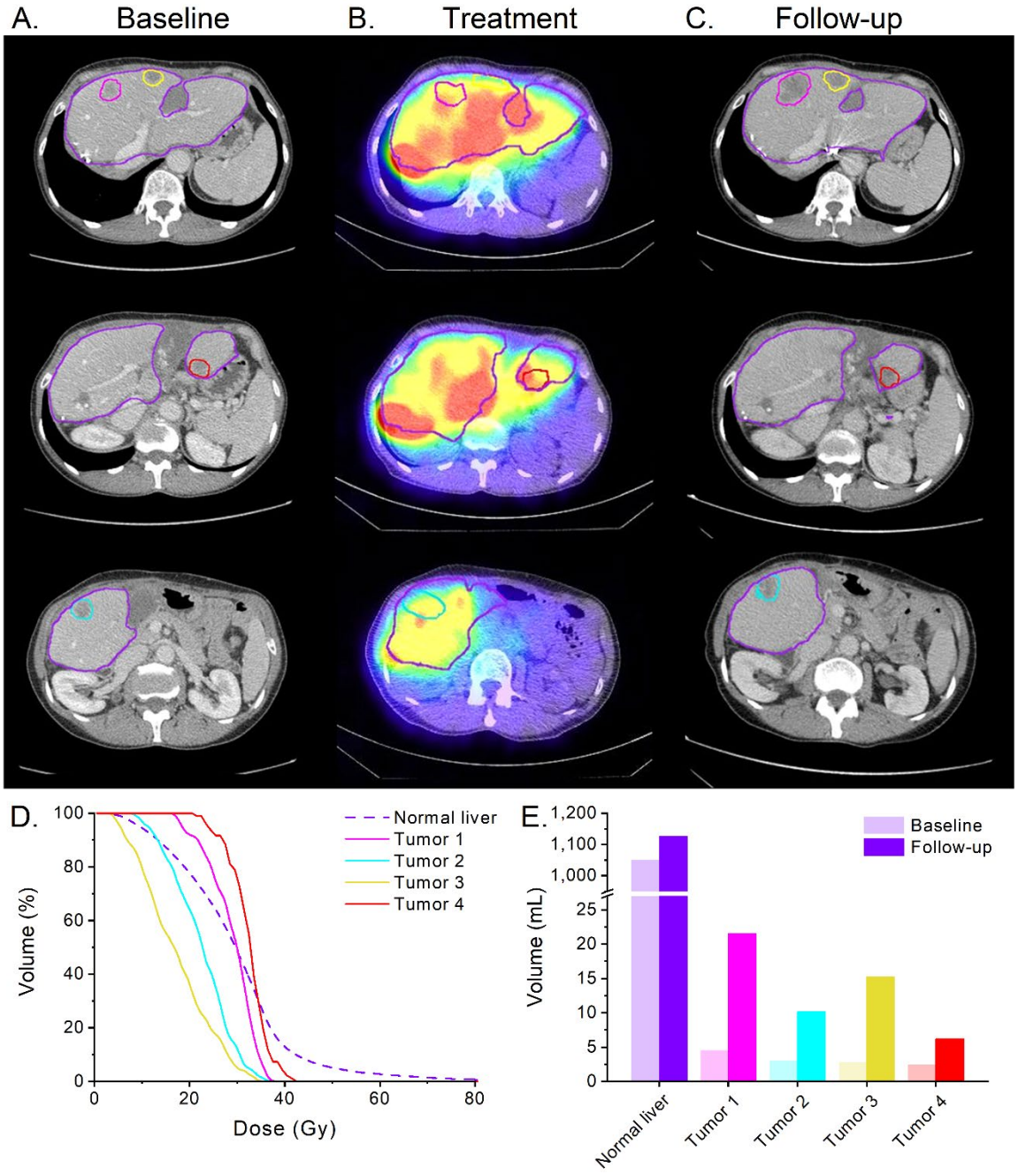

Supplemental Figure 2: Patient 18 (66 y, 1.53 m^2 BSA): rectal cancer. The primary tumor was resected and the patient received two lines of prior chemotherapy. (A) Baseline imaging acquired 13 days prior to SIRT showed PD. ^{99m}Tc-MAA, angiography and coil embolisation were performed to optimally redirect flow away from lungs to achieve 0% lung shunt. ^{90}Y microspheres were administered in a single injection of 847 MBq. (B) SPECT/CT one day post-SIRT demonstrated a poor uptake distribution (C) CT imaging 77 days following SIRT revealed a significant increase in tumor volume. (D) DVH of absorbed doses highlight greater doses in normal liver compared to tumor, in particular, tumors 2 and 3. (E) Volumetric response illustrates PD in all tumors.

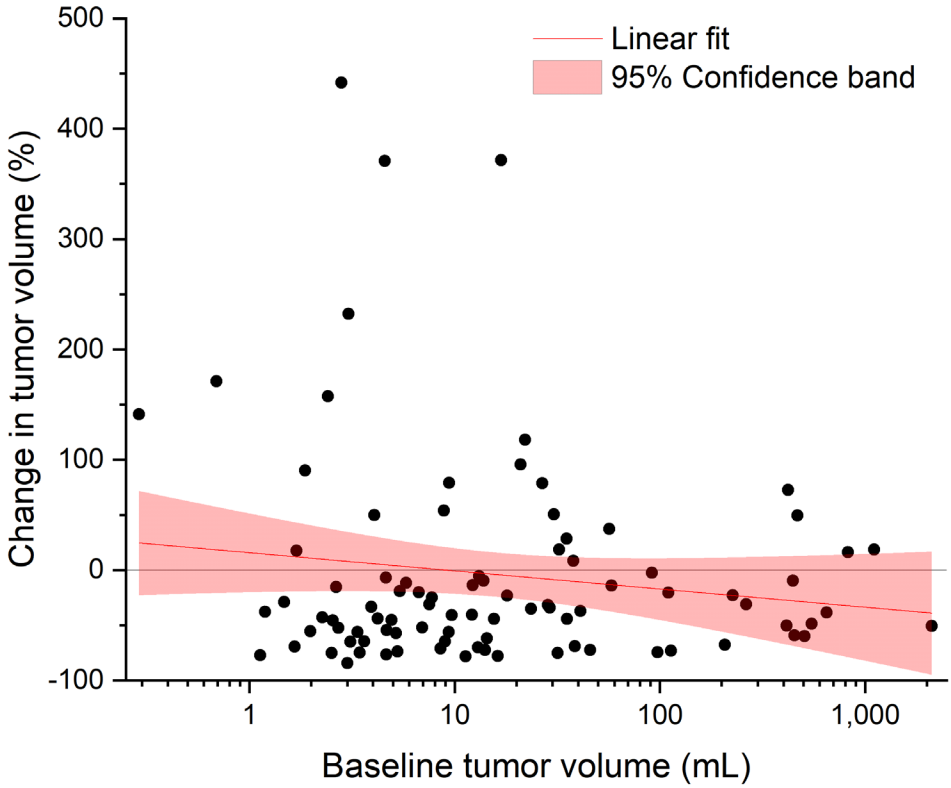

Supplemental Figure 3. Relationship between baseline and 3-month follow-up tumor volume. Linear regression (red line) with 95% CI (red band), shows no significant correlation (p=0.19, R^2=0.0013) between log baseline tumor volume and percentage change in tumor volume.